Target Velocity Estimation with FM and PW Echo Ranging Doppler Systems — Part II: Systems Analysis

Jens E. Wilhjelm, *Member, IEEE*, and Peder C. Pedersen, *Senior Member, IEEE*

***Abstract*—In Part I, Signal Analysis, of this paper, the encoding of the velocity and range information into the received and demodulated signals was discussed, based on transmission of coherent repetitive linear sweep signals. In Part II, two different implementations of FM Doppler systems are presented that can be used to obtain velocity profiles. The first implementation is similar to the implementation of a conventional pulsed wave (PW) Doppler system, based on measurement of phase shift (correlation based system); the second implementation is a frequency-domain analog to the PW Doppler system, based on time shift measurements (cross correlation-based system).**

I. Introduction

BLOOD velocity images can be obtained noninvasively by means of pulsed ultrasound. The basis for this is the Doppler effect that gives rise to a compression or expansion of the pulsetrain scattered by the red blood cells moving towards, or away from, the transducer. This compression or expansion results in a change in the pulse repetition interval which can be measured with PW Doppler either as a phase shift [1]–[3], [15] (PW-*psm* [22]) or a time shift [4]–[6], [9]–[12] (PW-*tsm* [22]).

One characteristic inherent in PW emission is the high peak to average power ratio. This is unavoidable in order to obtain a short pulse, and thereby, a high bandwidth. However, there are potential safety concerns due to the high peak power, such as the risk of introducing cavitation [16]. This high peak to average power ratio can be significantly reduced, without limiting the bandwidth, by transmitting coded signals. One kind of coded signal, coherent linear frequency modulated sinusoids, have particularly useful properties. Specifically, such excitation signals allow Doppler information to be extracted with either phase shift measurement or frequency shift measurement (the latter being analogous to time shift measurement with PW Doppler). In evaluating ultrasound Doppler systems, one major performance index is the resolution cell size. The resolution cell size refers to the smallest flow volume that the Doppler system can resolve. It is defined by the axial resolution and by the lateral beam width at the range of interest; only the axial resolution size is controlled by the signal processing and thus quantified by the aforementioned performance index. This paper will discuss the two different signal processing techniques and determine this index.

Manuscript received December 12, 1992; revised April 12, 1993; accepted April 14, 1993. This work was supported by the National Science Foundation under Grant BCS-9009886, by the Danish Research Academy, and by the Knud Hojgaards Foundation, Denmark.

J. E. Wilhjelm was with the Biomedical Engineering Department, Worcester Polytechnic Institute, Worcester, MA. He is now with the Electronics Institute, Technical University of Denmark, DK-2800 Lyngby, Denmark.

P. C. Pedersen is with the Electrical and Computer Engineering Department, Worcester Polytechnic Institute, Worcester, MA 01609.

IEEE Log Number 9210312.

II. Assumptions and Definitions

The two previously mentioned signal processing methods are evaluated, based on a single moving scatterer. The transmitted sweep signals have rectangular envelopes which allow simple formulation of features such as Doppler induced sweep rate and range sidelobes. However, the spectra of the PW and FM excitation signals cannot be matched, reducing the validity of a strict performance comparison. In a future paper, Gaussian envelope functions will be applied to the transmitted signals in order to match the PW and FM spectra.

We define an *acoustic particle* to be a point scatterer which reflects a replica of the transmitted signal back towards the transducer. The backscattering coefficient is assumed to be independent of frequency. The medium between the acoustic particle(s) and the transducer is considered isotropic with no attenuation.

The excitation signal for the FM Doppler systems is a repetitive sweep where each sweep signal has the length t_m, as illustrated in Fig. 1(b). The sequence of sweeps are numbered 0 to $L-1$. Its frequency increases linearly from frequency f_1 to frequency f_2. The mean frequency of the signal is $f_0 = (f_1 + f_2)/2$. This signal is transmitted by a transducer every T_r seconds. Concurrent with the transmission, an adjacent transducer receives echoes from acoustic particles located inside the region where the transmit/receive beams overlap. For simplicity, the transducer bandwidths are assumed infinite, and it is further assumed that the transmit and receive beams overlap completely. This can be approximately achieved with a two-element annular array. A single moving particle is considered, located at the depth d in the vicinity of the nominal depth D, at $t = 0$ and $n = 0$, and traveling as indicated in Fig. 1(a). Beam intensity modulation is ignored. The received signal, due to two consecutive transmissions, is shown in Fig. 1(b).

Note that PW excitation is obtained by setting $f_1 = f_2 = f_0$, where f_0 now corresponds to the mean frequency of the burst signal, and by letting t_m be much smaller than for the FM case.

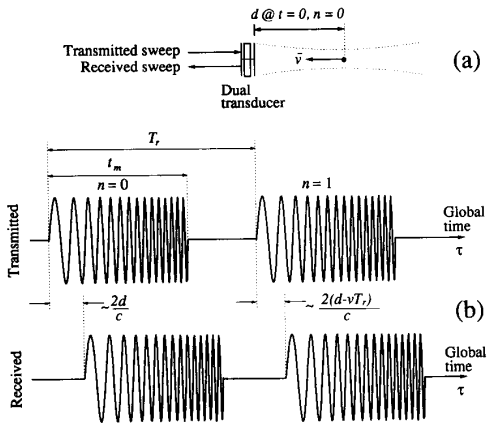

Fig. 1. (a) Conceptual illustration of dual transducer transmitting and receiving a sweep. An acoustic particle, located at $d \cong D$ at $t = 0$ and $n = 0$, is travelling towards the transducer with velocity $\bar{v}$. (b) Illustration of two transmitted sweeps and the corresponding Doppler compressed and shifted sweeps received from the acoustic particle.

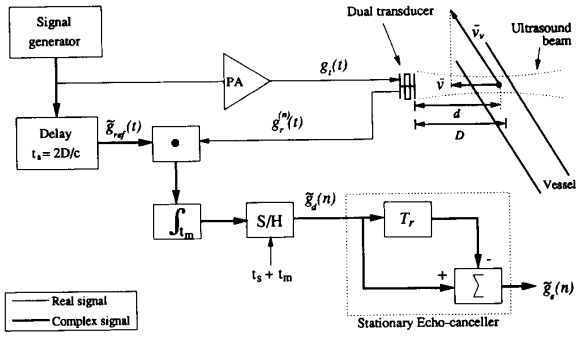

Fig. 2. Block diagram of a correlation-based general Doppler system applicable for PW, random noise, pseudorandom noise, and FM signals (the latter will be discussed in the text). The system utilizes a dual transducer. The received signal is multiplied with a complex time delayed version of the transmitted signal. The multiplier output is next integrated and the result is sampled. The result yields the so-called sampled Doppler signal $\tilde{g}_d(n)$ This Doppler signal may then be high-pass filtered to remove stationary echo components.

III. Phase Shift Measurement System

In this section, the theory of operation for the *psm* signal processing method will be described. Then, the resolution cell together with the Doppler spectrum will be characterized based on this signal processing method.

The continuous wave Doppler [1], the PW-*psm* Doppler, and Doppler systems using random [14] or pseudorandom [7], [8] excitation signals are all based on a *correlation* approach [15]. Such a general Doppler system is shown in Fig. 2.

In Fig. 2, each received signal is multiplied with $\tilde{g}_{\text{ref}}(t)$ which is a delayed analytic replica of the transmitted signal. The output of this multiplier is integrated over the time duration of the transmitted signal. The result of each integration is sampled and these samples constitute the so-called Doppler signal which will oscillate with the Doppler frequency. A system that implements this kind of processing is also called a *correlation system* [15] but to avoid confusion the term will not be used in this paper since a cross correlation-based Doppler system will be introduced later. It will now be demonstrated that the signal processing scheme shown in Fig. 2 is applicable with FM excitation, and the implications of using such signals will be analyzed.

Consider a single acoustic particle located at the depth d at $t = 0$ and moving with the velocity $\bar{v}_v$. The magnitude of the velocity component along the acoustic axis of the transducer is v. By observing Fig. 2 it is seen that each point on the sampled Doppler signal, $\tilde{g}_d(n)$, is obtained after the integration is completed at $t = t_s + t_m$. Thus the Doppler signal has the form

$$\tilde{g}_d(n) = \int_{t_s}^{t_s+t_m} \tilde{g}_{\text{ref}}(t)\, g_r^{(n)}(t)\, dt \tag{1}$$

where $t_s = 2D/c$ is the round trip delay to the nominal depth, D, and t_m is the duration of the sweep. $\tilde{g}_r^{(n)}(t)$ refers to the received signal in response to the nth consecutive transmitted sweep. t_m and t_s are measured in local time, i.e., $t = 0$ at the onset of each transmitted sweep. Basically, the two signals in the integrand in (1) are both delayed versions of the transmitted signal: the received signal, $g_r^{(n)}(t)$, will have experienced a delay equal to the round trip travel time from transducer to the moving particle. The delay is $2d^{(n)}/c$, where $d^{(n)} = d - vnT_r$ and T_r is the sweep repetition time. The reference signal has been delayed by t_s. Incorporating the expressions for these delays, (1) can be written as [19]:

$$\tilde{g}_d(n) = A \int_{t_s}^{t_s+t_m} \tilde{g}_t\left(t - \frac{2D}{c}\right) g_t\left(\beta\left(t - \frac{2(d+nvT_r)}{c+v}\right)\right) dt \tag{2}$$

where A is a constant containing all the relevant amplitude factors, such as backscatter coefficient, and where $\beta = (c+v)/(c-v)$ is the Doppler compression/expansion factor. Ignoring the Doppler compression/expansion of the individual received sweeps (i.e., $\beta = 1$ and $c + v \cong c$), using $t_s = 2D/c$ and substituting $t' = t - t_s$ gives

$$\tilde{g}_d(n) = A \int_0^{t_m} \tilde{g}_t(t')\, g_t\left(t' - \frac{2(d+nvT_r)}{c} + t_s\right) dt'. \tag{3}$$

Now substituting $\tau_n = t_s - 2(d + nvT_r)/c$ makes it possible to write (3) as a function of τ_n as follows:

$$C(\tau_n) = A \int_0^{t_m} \tilde{g}_t(t') g_t(t' + \tau_n) dt' \tag{4}$$

where τ_n is a discrete function of n; τ_n represents the *difference* between the fixed delay, t_s, and the round trip travel time at the nth transmission. Note that (4) is derived for a single acoustic particle. Mathematically, (4) indicates that the system in Fig. 2 determines a single value in the autocorrelation function of the transmitted signal for each transmission. It should be noted that as $\tilde{g}_t(t')$ and $g_t(t' + \tau_n)$ become increasingly uncorrelated with increasing τ_n, the sampled output of the integrator tends towards zero. This is the basis for obtaining information at a selected range with this system. Of course, if the particle, for $n = 0$, is located

at the depth $d = D$, the two delays, t_s and $2d/c$, will be equal so that the two input signals to the mixer will be in phase (assuming that the Doppler compression/expansion on the individual received signals can be ignored). In the next two subsections it will be shown that the axial extent of the resolution cell is obtained from the envelope of $\tilde{g}_d(n)$, and that $\tilde{g}_d(n)$ will oscillate with the Doppler frequency.

The last signal processing block in Fig. 2 is a stationary echo canceller (SEC). This implementation of a SEC is the simplest way to remove signals originating from stationary and/or quasi-stationary structures. However, many other types of high-pass filters have been used with the PW-*psm* system, and the SEC is included here to make the system in Fig. 2 functionally similar to the FM-*fsm* system, to be presented later.

A. Range Resolution Size

The range resolution size is obtained by observing the envelope of the receiver output, $\tilde{g}_d(n)$, versus time for a single acoustic particle moving axially along the center of the beam. Specifically, the range resolution size is calculated from the time interval between the –3-dB values of the envelope of $\tilde{g}_d(n)$ and the known velocity of the acoustic particle.

The range resolution results will be based on numerical modeling, thereby avoiding the approximations incurred by ignoring the Doppler effect. In order to highlight the effects of using FM signals, the range resolution for the FM-*psm* Doppler will be compared with that of the PW-*psm* Doppler. This comparison will be done using excitation signals with a rectangular envelope. This means that the shapes of the spectra of the two excitation signals are different, but the parameters have been chosen so that the bandwidths are roughly similar.

Consider the following parameters: $D_{\max} = 100$ mm, $L = 128$, $D = 50$ mm, $T_r = 2D_{\max}/c = 133.3$ μs, $T_{\text{obs}} = T_r L = 17.07$ ms, where L specifies the number of transmissions. The particle moves with the velocity $v = 0.5$ m/s in direction of the transducer and is placed so that it moves from a depth $d = D + \Delta d$ to a depth $d = D - \Delta d$. The initial location of the particle is, therefore, $d^{(0)} = D + T_{\text{obs}} v/2 = 54.27$ mm. For the FM system $f_1 = 2.5$ MHz, $f_2 = 3.5$ MHz, and $t_m = 0.8T_r = 106.6$ μs. For the PW system $f_0 = 3$ MHz, $p = 4$ (where p is number of cycles in one burst) and $t_m = 4/f_0 = 1.33$ μs.

The upper part of Fig. 3 shows the position of the particle as a function of time from the onset of the first transmission. The lower part shows the real part of the discrete Doppler signal ($\tilde{g}_d(n)$), as given in (2), for the FM-*psm* Doppler together with the associated envelope. For comparison, Fig. 3 also shows the corresponding envelope for the above mentioned PW-*psm* system. The two discrete correlation curves for FM and PW Doppler contain 128 samples each (as $L = 128$), and each sample point is a result of correlating the reference signal and the received signal, as specified in (2). Each time that the transmission of a new signal starts, the particle has moved the additional distance vT_r towards the transducer, corresponding to a change in round trip travel time of $2vT_r/c$. The shape of the envelope of the Doppler signal corresponds to the signal amplitude received from an acoustic particle

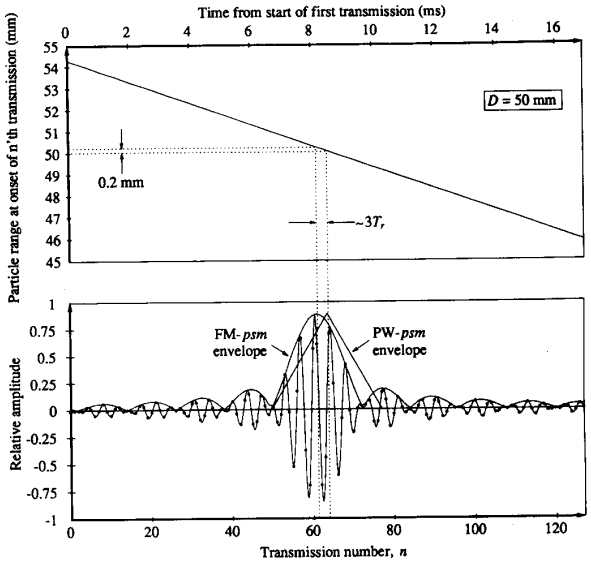

Fig. 3. Upper panel: The position of the particle as a function of time since start of transmissions. Lower panel: The real part of the discrete Doppler signal for the FM-*psm* system as well as the envelope of the FM and the PW Doppler signals from a single particle traveling with the velocity $v = 0.5$ m/s directly towards the transducer. $D = 50$ mm. In this ideal situation, the envelopes are nearly identical to the envelope of the autocorrelation function of the transmitted signal. The two range cells do not completely overlap. See text for details.

at different depths in the vicinity of D. Thus the envelope represents the amplitude sensitivity along the acoustic axis of the measurement system. The –3-dB width of the main lobe will be defined as the *minimum range resolution size.*

From Fig. 3 it is observed that the resolution cells are fairly similar. However, the FM resolution cell features *range sidelobes*, and the acoustic particle position producing a maximum output is shifted relative to the position of the PW resolution cell.

As the particle moves the distance $vT_{\text{obs}} = 8.5$ mm during T_{obs}, the –3-dB size of the FM and the PW resolution cells can be found directly from Fig. 3 to be approximately 0.75 and 0.6 mm, respectively. The general equation [1] for minimum obtainable range resolution cell size is

$$\Delta D_{\min} \cong \frac{c}{2B_{\text{FM}}}. \tag{5}$$

Equation (5) predicts a result similar to what was found in Fig. 3, if $B_{\text{FM}} \cong f_2 - f_1$ for the FM Doppler (valid since $1/t_m \ll f_2 - f_1$) and $B_{\text{FM}} \cong 1/t_m$ for the PW Doppler. It should be noted that somewhat different values are obtained if the transmitted signals are weighted with a Gaussian envelope.

The range sidelobes are a consequence of using coded signals, and only PW systems are completely free of range sidelobes. It is seen that the first sidelobe is about 13.4 dB below the main lobe. For the chosen parameters, the center of the first sidelobe is displaced about 1.1 mm from the center of the main lobe. Note, however, that the range side lobes may be reduced by changing the rectangular envelope function to a smoother function, such as a Gaussian function, which is also

a more realistic representation of the envelope function from an actual transducer, due to its bandlimited response.

The small shift of the position of the FM-*psm* resolution cell relative to the true acoustic particle location is due to the strong coupling between range and velocity information that is present with linear FM excitation signals. Specifically, the shift of the resolution cell is caused by the Doppler compression or expansion of the received signals which creates a Doppler shift of the initial transmission frequency *and* a Doppler shift of the sweep rate. As the range of the particle is coded as frequency, these two frequency shifts translate into a range shift. In the above system, the reference signal and the received signal in (1) will never be able to correlate perfectly as their instantaneous frequency functions, $\Psi_{\text{ref}}(t)$ and $\Psi_r^{(n)}(t)$, respectively, differ slightly. This is clearly illustrated in [22, fig. 3]. Assuming that $d^{(0)} = D$, the correlation function is maximum when $\Psi_r^{(0)}(t)$ is time-shifted by Δt_{match} such that $\Psi_{ref}(t_{mp,\text{ref}}) = \Psi_r^{(0)}(t_{mp,r} - \Delta t_{\text{match}})$. $t_{mp,\text{ref}}$ and $t_{mp,r}$ are the times that corresponds to the midpoints of $\Psi_{\text{ref}}(t)$ and $\Psi_r^{(n)}(t)$, respectively. As seen from [22, fig. 3], this requires that

$$\frac{2d}{c+v} + \frac{t_m}{2\beta} = \frac{2D}{c} + \frac{t_m}{2} + \Delta t_{\text{match}} \tag{6}$$

where Δt_{match} has been calculated to be approximately $(2v/c)(f_1 + f_2)/(2S_0)$[18]. Isolating $d - D$ in (6) yields the range offset where the best correlation is obtained. Some manipulation of (6) gives

$$d - D \cong v\left[\frac{D}{c} + \frac{f_2}{f_2 - f_1}t_m\right] \tag{7}$$

where it can be seen that this range offset is proportional to velocity of the particle. With the parameters used previously and $c = 1500$ m/s, we obtain $d - D \cong 200$ μm. As the particle moves $vT_r \cong 66.7$ μm between consecutive sweeps, the displacement will correspond to approximately $3T_r$, as shown in Fig. 3. The upper bound for (7) can be found at $D = D_{\max}$ and $t_m = T_r$. Inserting these parameters in (7), together with the so-called aliasing velocity (to be defined subsequently in (10)) and using 100 % relative bandwidth (i.e., $f_0 = f_2 - f_1$, where $f_0 = (f_1 + f_2)/2$) yields

$$(d - D)_{\max} \cong \frac{c}{f_2 - f_1}. \tag{8}$$

If B_{FM} is substituted for $f_2 - f_1$ in (8), then $(d - D)_{\max}$ is seen to be approximately equal to the minimum resolution cell size, ΔD_{min}, as given in (5).

B. Doppler Spectrum

Next consider the spectrum of the Doppler signal in (1). When the particle moves along the axis of the acoustic beam, the arrival time of the received signal changes correspondingly. This will make the sampled output of the integrator oscillate at the Doppler frequency. This has been demonstrated for random signal excitation [7], [14] and we have specifically verified this for FM (and PW) excitation [19]. Specifically, by solving (3) for the case where $D \cong d$ and ignoring the second-order

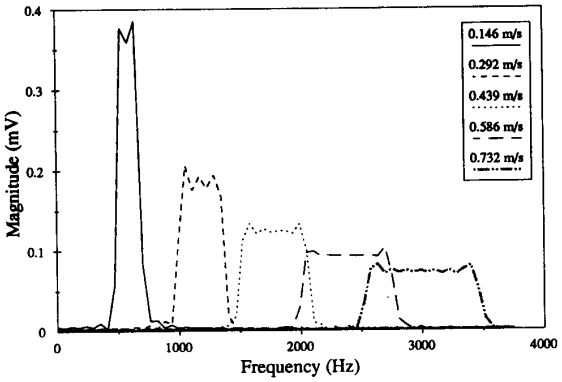

Fig. 4. Doppler spectra obtained with the FM-*psm* Doppler system for five different particle velocities. Only one moving particle is considered. The width of the spectrum increases with velocity (as the transit time decreases with increasing velocity). As 128 transmissions are used, only particles with velocity less than $2\Delta D/T_{\text{obs}} = 0.11$ m/s will be included in the entire Doppler signal.

effects, it is found that the Doppler signal prior to the SEC can be written approximately as

$$\tilde{g}_d(n) \cong \exp\left\{j\left[2\pi\frac{2v}{c}\left(\frac{f_1 + f_2}{2}\right)(nT_r) + \varphi_{d,\text{FM}}\right]\right\} \tag{9}$$

where it is noted that the Doppler shift is related to the mean frequency of the transmitted signal. $\varphi_{d,\text{FM}}$ is a constant phase factor. As (9) is only valid for $d \cong D$, it does not describe the range cell shape function shown in Fig. 3. In addition, if $\tilde{g}_d(n)$ had been calculated from (2), a sweep component would be present in (9). However, in this case $\tilde{g}_d(n)$ cannot be found in a closed form when the transmitted signal has a rectangular envelope. The sweep term originates from the fact that the Doppler signal is based on the cross-correlation between two sweeps with differing sweep rates [18]. In order to study the Doppler signal in (1) without the approximations in (9), numerical modeling must be applied. Using the system parameters listed in the beginning of Section III-A, the Doppler spectra in Fig. 4 have been obtained. These spectra are based on a single acoustic particle traveling at different typical blood velocities, using a 128 point DFT of the expression of the discrete Doppler signal $\tilde{g}_d(n)$ in (1). In Fig. 4 a spectral broadening in the form of a sweep component is noted.

The following general observations can be made: as the Doppler signal in Fig. 3 for the FM-*psm* system is longer — or, equivalently, exists for a wider range of particle locations around D — than the corresponding Doppler signal for the PW-*psm* system, the spectral broadening due to transit time is smaller for the FM-*psm* system. However, this effect is somewhat counteracted by the sweep component in the (FM-*psm*) Doppler signal which broadens the spectrum. From computer simulations we have found that the width of the Doppler spectra are roughly identical for both FM and PW. A more rigorous comparison requires, however, that the systems have identical bandwidths of the transmitted signal. Nevertheless, the velocity uncertainty based on the spectral width is very similar for the two systems.

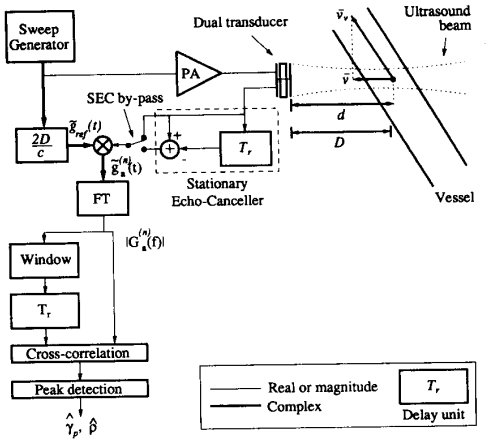

Fig. 5. Block diagram of FM-*fsm* system. Repetitive chirps are generated with a sweep generator and transmitted via one element of a dual transducer. The other element of the transducer receives the backscattered acoustic signals and delivers the electrical signals to a SEC. The echo-cancelled signal is demodulated and transformed into the frequency domain. Consecutive windowed magnitude spectra are cross correlated to estimate the frequency shift.

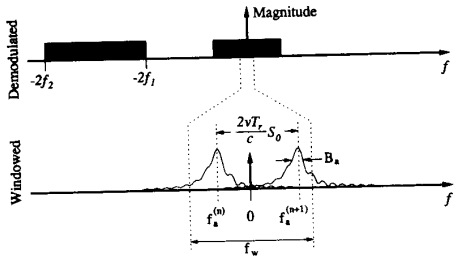

Fig. 6. Conceptual illustration of the spectra appearing in the FM-*fsm* system. The top part shows the envelope of the spectrum of the demodulated signal. The spectra associated with the difference frequency are called *fsm* spectra. The bottom part shows two consecutive *fsm* spectra for one particle. The spectral shift between the two spectra is exaggerated for clarity. The spectral window length, f_w, that defines the range resolution size is indicated as well. Note that the *fsm* spectra are not fully contained within the spectral window.

Finally, the aliasing velocity has been found to be [19]

$$v_{\text{alias}} = \frac{c^2}{8\, D_{\max} \frac{f_1+f_2}{2}}. \tag{10}$$

The velocity aliasing can be circumvented by changing the coding of consecutive transmission signals so that two, or more, consecutive transmitted signals correlate to a very low degree. This permits the pulse repetition frequency, $1/T_r$, to be increased without range aliasing, that is, without interpreting an echo from a range $cT_r/2 + \Delta d$, as coming from the range Δd. This has been demonstrated by Cathignol [7], [8], but further consideration of this is outside the scope of this paper.

IV. Frequency Shift Measurement System

The *FM-fsm Doppler system* is the FM counterpart to the PW-*tsm* Doppler system. The block diagram and pertinent spectra are shown in Figs. 5 and 6, respectively. The sweep parameters and transducer characteristics are the same as for the FM-*psm* Doppler system and were described in Section II. A single moving particle is considered, located at the depth d in the vicinity of the nominal depth D, at $t = 0$, and traveling as indicated in Fig. 5.

Consecutive received signals can be subtracted in the SEC *which is by-passed in the following systems analysis*, but will be discussed in a later paper. When the SEC is incorporated, the FM-*fsm* Doppler system requires a coherent sweep generator, i.e., a sweep generator where all the consecutive sweep signals start at the same phase value.

The received signal is multiplied in quadrature with a delayed analytic version, $\tilde{g}_{\text{ref}}(t)$, of the sweep signal. The transmitted signal is the real part of this analytic signal (apart from the gain factor of the power amplifier), as seen from Fig. 5. By means of the delay, the depth of interest, D, is selected for a given resolution cell. By multiplying the received sweep with the delayed sweep, followed by an Fourier transform, two distinct spectral components will arise, as seen in Fig. 6: a component around $f = 0$, produced by the difference frequencies, and a component produced by the sum frequencies which is located in the interval $[-2f_2; -2f_1]$. The spectral component due to the difference frequencies (here obtained from only one particle) — with SEC off — will be called the *fsm* spectrum; the sum spectrum is not used in the further processing.

The magnitude of the *fsm* spectrum (the phase is not considered) will, around $f = 0$, contain information from a region around the depth D. Specifically, the frequency axis can be considered a linear transformation of the range axis (axial distance from the transducer). This can be seen from the fourth term in (17) in [22]. An acoustic particle located at depth d results in a round trip travel time of $2d/c$, which in turn produces a frequency shift, relative to the demodulated signal, of $(2(D-d)/c)S_0$ where S_0 is the sweep rate in hertz per second. Thus the range (relative to D) to frequency conversion is

$$f = \frac{2(D-d)}{c} S_0. \tag{11}$$

Hence, the depth $d = D$ corresponds to $f = 0$, and range values of d smaller than D yield positive frequencies. A rectangular spectral window of the width f_w, applied around $f = 0$, determines the axial extent of the range cell. This is illustrated in Fig. 6. Adjacent range cells can be envisioned to the right and left of the one in Fig. 6. The fact that the spectral window, f_w, may truncate the *fsm* spectra introduces a form of *range sidelobes* in the receiver characteristics. The windowed magnitude spectrum, due to the nth received signal, is given as

$$|G^{(n)}_{a,w}(f)| = \left\{ \begin{array}{cc} |G^{(n)}_a(f)| & -f_w/2 \le f \le f_w/2 \\ 0 & \text{otherwise} \end{array} \right\}. \tag{12}$$

This windowed magnitude spectrum, in a manner similar to the time-domain cross correlation done in the PW-*tsm* Doppler system, is cross correlated with the magnitude spectrum obtained from the next received signal. The cross correlation is given in (13) for the nth and the $(n+1)$th transmissions

where γ is any frequency shift:

$$C^{(n),(n+1)}(\gamma) = \int_{\infty}^{-\infty} \{|G_{a,w}^{(n)}(f)| - < |G_{a,w}^{(n)}(f)| >\} \{|G_a^{(n+1)}(f+\gamma)| - < |G_a^{(n+1)}(f+\gamma)| >\} df \tag{13}$$

where $< \cdot >$ indicates mean value; thus (13) is calculating the cross covariance. Assuming that the magnitude spectra are nearly identical, the cross correlation function will resemble the autocorrelation function of one *fsm* magnitude spectrum, shifted an amount, $\hat{\gamma}_p$, equal to the spectral shift between the magnitude spectra. This cross correlation function, therefore, has a unique maximum at the frequency shift $\hat{\gamma}_p$, as expressed in (14), which represents the best estimate of the true frequency shift γ_p:

$$C^{(n),(n+1)}(\hat{\gamma}_p) = \max_{\gamma}[C^{(n),(n+1)}(\gamma)]. \tag{14}$$

Using [22, eq. (22)], the estimated velocity of the particles, $\hat{v}$, in the vicinity of D can be determined from $\hat{\gamma}_p$ as follows:

$$\hat{v} = \frac{\hat{\gamma}_p c}{2T_r S_0}. \tag{15}$$

In case of multiple particles, the superposition principle can be used to find the resulting *fsm* spectrum as a complex summation of the *fsm* spectra from each particle. This is analogous to the formation of the received time-domain signal in PW Doppler systems. The PW and FM Doppler systems each obtain waveforms with a "signature" formed by the specific arrangement of the acoustic particles within the resolution cell. For the PW Doppler the waveform is a time-domain signal whereas for the FM-*fsm* Doppler the waveform is a frequency spectrum. The waveforms are shifted in their respective domains from one transmission to the next. Clearly, the signal processing scheme for the FM-*fsm* Doppler takes place in the frequency domain instead of in the time domain as is the case for the PW-*tsm* Doppler.

We note that we are measuring the displacement ($\Delta d = vT_r$) of the particles directly. As the *fsm* magnitude spectra (obtained from consecutive received signals) are cross correlated, the FM-*fsm* Doppler technique should be less affected by the frequency dependent factors such as attenuation and scattering than the FM-*psm* Doppler system where correlation takes place between the received signal and delayed versions of the transmitted signal. It has been noted that the PW-*tsm* Doppler system has the same advantage over the PW-*psm* Doppler system [5].

From the previous discussion, we can conclude that there is a direct analogy between the PW-*tsm* and the FM-*fsm* Doppler systems. The *fsm* spectrum originates from the demodulated signal, described by [22, eq. (12)]; this signal is itself a chirp. From this it can be seen that the position of the spectrum relative to $f = 0$ is related to both velocity and range as was the case for the FM-*psm* Doppler. However, the *frequency shift* between the *fsm* magnitude spectra from two consecutive received signals is unaffected by range. The width of the *fsm* spectrum, B_a, defines the minimum range resolution and is related to the duration of the transmitted signal and the Doppler sweep rate; the latter was defined in [22, eq. (16)]. Subsequently, the range resolution size will be discussed in detail. The velocity uncertainty, on the other hand, can only be adequately described when based on a realistic form of the transmitted signal, and will, therefore, be considered in a future paper.

A. Range Cell Size

In Fig. 6 two consecutive typical *fsm* magnitude spectra for a single particle are indicated. The center of the nth *fsm* spectrum is given in [22, eq. (18)], as

$$f_a^{(n)} = \frac{2v}{c} f_1 + 2D\frac{v}{c^2} S_0 + 2\frac{D-d}{c} S_0 + 2\frac{vnT_r}{c} S_0 + S_d \frac{t_m}{2} \cong 2\frac{D-d}{c} S_0 \tag{16}$$

where the last simplification indicates the approximate position of the spectrum when the influence from particle velocity is removed. Ignoring the Doppler compression/expansion (i.e., $S_d = 0$), the demodulated signal becomes a tone of length t_m. The width of the (*fsm*-) spectrum, B_a, measured at the –4-dB level, is approximately $1/t_m$. Now the minimum obtainable resolution size is typically defined as the minimum distance between two reflectors that allows them to be distinguished. Conventionally, this distance is obtained when the two *fsm* spectra are separate with a frequency spacing of B_a. Computing the distance, corresponding to the frequency shift B_a, gives

$$\Delta D_{\min} = \frac{c}{2S_0} B_a \cong \frac{c}{2S_0}\frac{1}{t_m} = \frac{c}{2(f_2 - f_1)} \tag{17}$$

which is identical to the general expression for the *minimum* axial resolution size for an echo-ranging system, given in (5). Including the width of the spectral window, f_w, the axial dimension of the resolution cell is

$$\Delta D \cong \frac{c}{2S_0}\left(f_w + \frac{1}{t_m}\right) = \frac{1}{2}\left(\frac{f_w}{S_0} + \frac{1}{f_2 - f_1}\right)c. \tag{18}$$

The expression for ΔD for the PW-*tsm* Doppler system is similar to (18)[19].

However, if the Doppler compression/expansion is considered, $S_d \neq 0$. Then the width of the *fsm* spectrum, B_a, will be slightly larger than predicted previously. Specifically, B_a will become a complicated function of t_m and $(f_2 - f_1)$ [17]; however, the approximation $B_a \cong 1/t_m$ can be made in case $1/t_m \ll S_d t_m$ or, equivalently, $(4v/c)(f_2 - f_1)t_m \ll 1$. Note that this analysis does not consider the range sidelobes present in the *fsm* spectrum.

B. Range Offset Due to Velocity

The range offset is due to the strong coupling between range and velocity and is linearly related to the velocity dependent terms in (16), i.e., the first, second, and fifth term. Calling the sum of these terms $\Delta f(v)$ gives

$$\Delta f(v) \cong \frac{2v}{c} f_1 + 2D\frac{v}{c^2} S_0 + S_d \frac{t_m}{2} = \frac{2v}{c}\left(f_1 + \frac{D}{c} S_0 + (f_2 - f_1)\right). \tag{19}$$

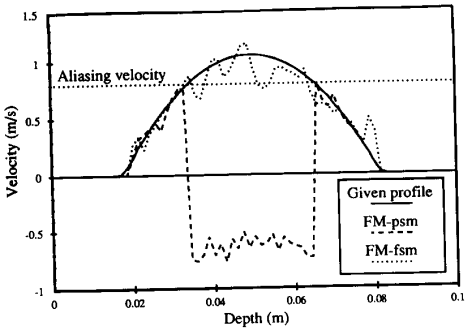

Fig. 7. Given velocity profile and simulation based velocity profiles for FM-psm and FM-fsm Doppler systems (see text for details). The calculated aliasing velocity in the FM-psm Doppler system is indicated.

Converting $\Delta f(v)$ to the corresponding range offset, $\Delta d(v)$, gives

$$\Delta d(v) = \Delta f(v)\frac{c}{2S_0} = \frac{v}{S_0}\left(f_1 + \frac{D}{c}S_0 + (f_2 - f_1)\right). \quad (20)$$

For $D = D_{\max} = T_r c/2$, $t_m = T_r$ and $f_2 - f_1 = (f_1 + f_2)/2$, an upper limit for the above offset can be written as

$$\Delta d_{\max} = 2vT_r \quad (21)$$

In conclusion, the maximal position offset equals the displacement of the particle during two pulse repetition periods. To minimize the effect of offset in the position estimate due to the velocity terms, the majority of the particles must stay inside the resolution cell during several pulse repetition periods, say 10 periods. However, this is also a requirement for maintaining sufficient coherence between consecutive *fsm* spectra [19].

V. Simulation Results

In order to provide a preliminary verification of the feasibility of velocity profiling with the FM-*psm* and the FM-*fsm* Doppler systems, a computer program [20] was developed to synthesize received sweep signals from acoustic particles moving with a parabolic velocity profile in a rigid tube. A 2-D simulation with a particle density of 50 particles/mm^2 was established. The estimated FM-psm and FM-fsm velocity profiles are shown in Fig. 7. A detailed performance analysis of the FM-fsm Doppler systems including experimental verification will be the topic of a forthcoming paper. Some experimental results can be found in [21].

The curves are based on the following parameters: the nominal frequency excursion of the transmitted signal span from $f_1 = 1$ to $f_2 = 6$ MHz. The chosen value of $t_m = 30$ μs yields $S_0 = 166.7$ GHz/s. The envelope of the transmitted signal is Gaussian and the –3-dB bandwidth can be calculated to be 1.4 MHz. $D_{\max} = 0.1$ m, $f_w = 653$ kHz, and $v_{\max} = 1$ m/s. The beamwidth was 2 mm. $T_r = 133.4$ μs. The number of transmissions, L, was 8. A SEC was used, but no stationary echoes were present. With these parameters the velocity aliasing begins at 0.8 m/s.

VI. Discussions and Conclusions

The underlying theory for the operation of the FM-*psm* and FM-*fsm* Doppler systems has been presented. The two systems have close counterparts in the PW-*psm* and the PW-*tsm* Doppler systems. The FM Doppler systems feature the advantage of long coded excitation signals which allows operation at low peak transmitted power, relative to PW Doppler systems. However, both FM Doppler systems exhibit range ambiguity in the form of so-called range sidelobes as well as a minor range cell displacement, proportional to velocity, due to the strong coupling between velocity and range information in the received signals. It is finally noted that these systems require a dual transducer.

As the FM-*psm* Doppler system is based on the correlation principle, and therefore, will display velocity aliasing at higher velocities, it does not have important advantages over other Doppler systems which are based on coded signals. On the other hand, as the FM-*fsm* Doppler system is based on measuring a frequency shift by cross correlating consecutive *fsm* spectra, velocity aliasing does not exist in this system. This is analogous to the PW-*tsm* Doppler system which measures a time shift by cross-correlating consecutive received signals. It will be the topic of a forthcoming paper to make quantitative performance comparisons between the FM-*fsm* and the PW-*tsm* Doppler systems.

References

[1] P. Atkinson and J. P. Woodcock, *Doppler Ultrasound and Its Use in Clinical Measurements*. London, U.K.: Academic, 1982.

[2] D. W. Baker, F. K Forster, and R. E. Daigle, "Doppler principles and techniques," in *Ultrasound: Its Applications in Medicine and Biology*. Amsterdam, The Netherlands: Elsevier Scientific, 1978, ch. III, pp. 161–287.

[3] W. D. Barber, J. W. Eberhard, and S. G. Karr, "A new time domain technique for velocity measurements using Doppler ultrasound," *IEEE Trans. Biomed. Eng.*, vol. BME-32, pp. 213–229, Mar. 1985.

[4] M. Bassini *et al.*, "An ultrasonic non-invasive blood flowmeter based on cross-correlation techniques," in *Proc. Ultrasonics Int. Conf.*, Graz, Austria, May 1979, pp. 273–276.

[5] O. Bonnefous and P. Pesqué, "Time domain formulation of pulse Doppler ultrasound and blood velocity estimation by cross-correlation," *Ultrason. Imaging*, vol. 8, no. 1, pp. 73–85, Jan. 1986.

[6] O. Bonnefous, "Statistical analysis and time correlation processes applied to velocity measurement," in *Proc. IEEE-UFFC Ultrason. Symp.*, Dec. 1989, pp. 887–892.

[7] D. J. Cathignol, "Signal-to-clutter ratio in pseudo random Doppler flowmeter," *Ultrason. Imaging*, vol. 8, no. 4, pp. 272–284, Oct. 1986.

[8] D. J. Cathignol, C. Fourcade, and J-Y. Chapelon, "Transcutaneous blood flow measurements using pseudorandom noise Doppler system," *IEEE Trans. Biomed. Eng.* vol. 27, pp. 30–36, Jan. 1980.

[9] D. Dotti *et al.*, "Blood flow measurements by ultrasound correlation techniques." *Energia Nucleare*, vol. 23, no. 11, Nov. 1976.

[10] P. M. Embree and W. D. O'Brien, "Volumetric blood flow via time-domain correlation: experimental verification." *IEEE Trans. Ultrason., Ferroelec., Freq. Contr.*, vol. 37, pp. 176–189, May 1990.

[11] S. G. Foster, P. M. Embree, and W. D. O'Brien, "Flow velocity profile via time-domain correlation: Error analysis and computer simulation," *IEEE Trans. Ultrason., Ferroelec., Freq. Contr.*, vol. 37, pp. 164–175, May 1990.

[12] S. G. Foster, "A pulsed ultrasonic flowmeter employing time domain methods," Ph.D. dissertation, Dept. of Elec. Eng., Univ. of Illinois, Urbana, IL, 1985.

[13] J. A. Jensen, "Stationary echo canceling in velocity estimation by time-domain cross-correlation," to be published.

[14] V. L. Newhouse and P. J. Bendick, "Analysis of random signal blood flow measurement," in *1973 IEEE Ultrasonics Symp. Proc.*, 1973, pp. 94–97.

[15] V. L. Newhouse, P. J. Bendick, and L. W. Varner, "Analysis of transit time effects on Doppler flow measurements," *IEEE Trans. Biomed. Eng.*, vol. 23, Sept. 1976.
[16] M. O'Donnell, "Coded excitation system for improving the penetration of real-time phase-array imaging systems," *IEEE Trans. Ultrason., Ferroelec., Freq. Contr.*, vol. 39, pp. 341–351, May 1992
[17] J. E. Wilhjelm, "Bandwidth of Gaussian weighted chirp," to be published.
[18] ——, "Cross-correlation functions of Gaussian weighted chirps," to be published.
[19] ——, "Ultrasound FM Doppler system for flow profiling with comparison to PW Doppler systems," Ph.D. dissertation, Dept. of Biomed. Eng., Worcester Polytechnic Institute, MA, 1991.
[20] J. E. Wilhjelm and P. C. Pedersen, "A generalized simulation approach to Doppler flow measurements," in *Proc. Ultrasonics Int. 91*, Le Touquet, France, June 1991, pp. 75–78.
[21] ——," FM Doppler systems — Experimental results," in *Proc. IEEE-UFFC Ultrasonics Symp.*, Dec. 1990, pp. 1553–1556.
[22] —— "Target Velocity Estimation with FM and PW Echo-Ranging Doppler Systems — Part I: Signal analysis," pp. 366–372, this issue.

Jens E. Wilhjelm (M'91), for a photograph and biography, please see page 372 of this issue.

Peder C. Pedersen (S'74–M'76–SM'87), for a photograph and biography, please see page 372 of this issue.